0022-3530/89 $3.00

An Exotic Eclogite/Blueschist Slice in a Barrovian-Style Metamorphic Terrain, Alanya Nappes, Southern Turkey

by ARAL I. OKAY

İTÜ, Maden Fakültesi, Jeoloji Bölümü, Ayazağa, İstanbul, Turkey

(*Received 18 December 1987; revised typescript accepted 15 July 1988*)

ABSTRACT

A 600 m thick, more than 40 km long slice of eclogite facies rocks, called the Sugözü Nappe, occurs in the Alanya area, southern Turkey, sandwiched between two other crystalline nappes which do not show H*P*/L*T* metamorphism. All three nappes were affected by a later Barrovian-type metamorphism and penetrative deformation which welded the nappes into a single tectonic unit. The Sugözü Nappe consists predominantly of garnet–mica schists with lenses of eclogite and blueschist metabasites. The mineral assemblage in the eclogites, garnet + omphacite + glaucophane + paragonite + quartz + phengite + rutile, is estimated to have formed at $13{\cdot}5 \pm 1{\cdot}5$ kb and 510 ± 25 °C. The eclogite assemblage is variably overprinted by a later Barrovian metamorphism with the development of barroisite, chlorite, and albite. The extent of the Barrovian overprint was controlled by the supply of fluid to the rocks.

The Barrovian metamorphism increases in grade downwards in the structural sequence; biotite and garnet isograds are mapped in the lowermost Mahmutlar Nappe, made up mostly of metapelites and metapsammites. The metapelites in the garnet zone consist of garnet + biotite + chlorite + muscovite + albite + oligoclase + quartz + ilmenite; metamorphic conditions are estimated as $6{\cdot}5 \pm 1{\cdot}0$ kb and 469 ± 13 °C.

The H*P*/L*T* rocks of the Sugözü Nappe underwent a cooling of about 100 °C during a dry uplift from a depth of about 48 km to 21 km where they were intercalated with the other nappes, and affected by a Barrovian metamorphism caused by the incoming fluids. The case of the Alanya Nappes illustrates that the Barrovian overprint observed in many eclogites and blueschists may not be due to increasing temperature during uplift, but simply due to the introduction of a fluid phase during part of the uplift *P–T* path.

INTRODUCTION

Blueschists overprinted by a lower pressure metamorphism are increasingly being recognized in Barrovian-style metamorphic belts (e.g., in the Dalradian, Gray & Yardley, 1979; in the Appalachians, Laird & Albee, 1981*a*). It is often not clear whether the entire Barrovian-style metamorphic belt has undergone the early H*P*/L*T* metamorphism, or whether the relict blueschists represent exotic metamorphic slices. The former alternative is consistent with the published thermal and tectonic models of metamorphism which involve an initial H*P*/L*T* metamorphism due to tectonic thickening by overthrusting, followed by a greenschist overprint due to the thermal relaxation through delayed and slowed uplift (e.g., England & Thompson, 1984). In contrast to these models, this paper describes an exotic blueschist/eclogite slice from the Barrovian-style metamorphic terrain of the Alanya Nappes, southern Turkey. The emplacement of this blueschist/eclogite slice was largely contemporaneous with the Barrovian-type metamorphism and penetrative deformation. Alanya blueschists are also of interest in that their protoliths were largely shallow-water sedimentery rocks, and they form a thin but continuous, rootless nappe.

GEOLOGICAL SETTING

The studied region lies within the Tauride tectonic unit which is made up of a pile of nappes mostly of sedimentary rocks and ophiolite, emplaced over a Mesozoic carbonate platform during the Late Cretaceous and Tertiary (Fig. 1; Brunn *et al.*, 1971; Şengör & Yılmaz, 1981). In the area studied, the highest structural unit is the Alanya Massif (Blumenthal, 1951) which comprises three superimposed nappes (Fig. 2; Okay & Özgül, 1984). Only the intermediate Sugözü Nappe, made up dominantly of garnet–mica schists, has undergone an early *HP/LT* metamorphism, whereas all the three nappes were affected by a later Barrovian metamorphism and deformation, which has welded the nappes into one unit, so that the contacts between the nappes are structurally conformable on the outcrop scale (Okay & Özgül, 1984). The lowermost Mahmutlar Nappe comprises metapelites, metapsammites, dolomites, metaquartzites, recrystallized limestones, and rare metabasites; part of this sequence is Permian in age (Özgül, 1985). The uppermost Yumrudağ Nappe is made up of a thick sequence of Upper Permian bauxite-bearing recrystallized limestones with a thin metaclastic unit at the base of the sequence (Fig. 2). Preliminary results of isotopic dating on the Alanya rocks indicate that both the early *HP/LT* metamorphism and the late Barrovian-type metamorphism are of Late Cretaceous age (M. Satır, pers. comm.).

Alanya Nappes tectonically overlie rocks of the Antalya Unit comprising mostly a strongly deformed and partially metamorphosed sequence of Palaeozoic and Mesozoic sedimentary rocks of passive continental margin type (Marcoux, 1978; Robertson & Woodcock, 1981; Özgül, 1985). In the Alanya region, rocks of the Antalya Unit occur in a large tectonic window, and in a narrow corridor between the Alanya Nappes and the relatively autochthonous Central Taurides (Fig. 1; Okay & Özgül, 1984; Özgül, 1985).

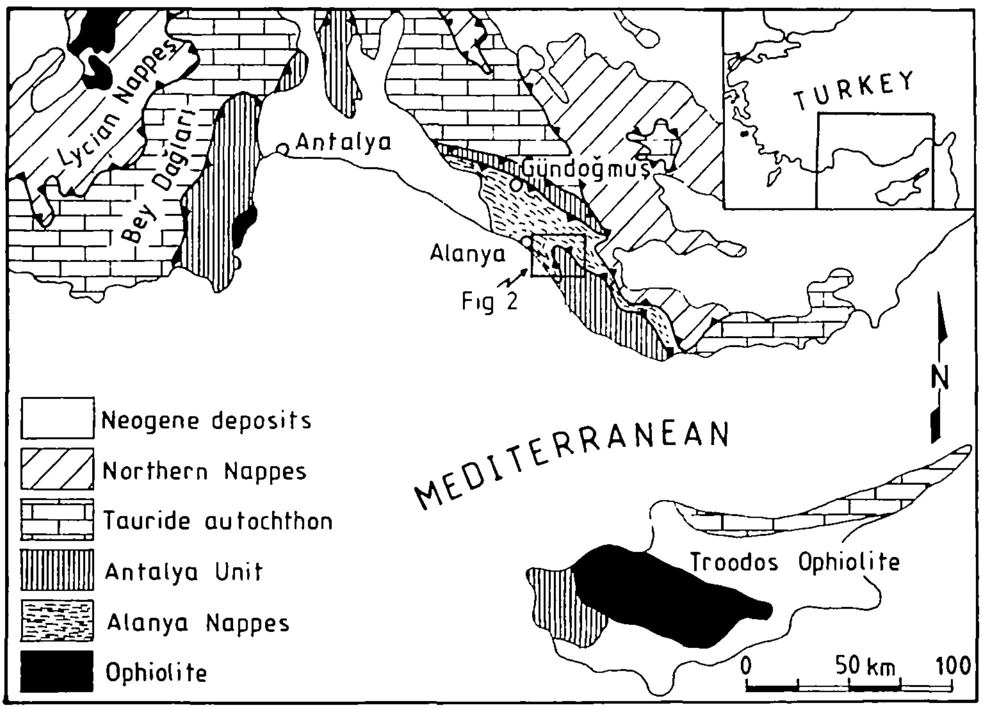

FIG. 1. Tectonic map of the western and central Taurides illustrating the regional setting of the Alanya Nappes. The area of Fig. 2 is also indicated.

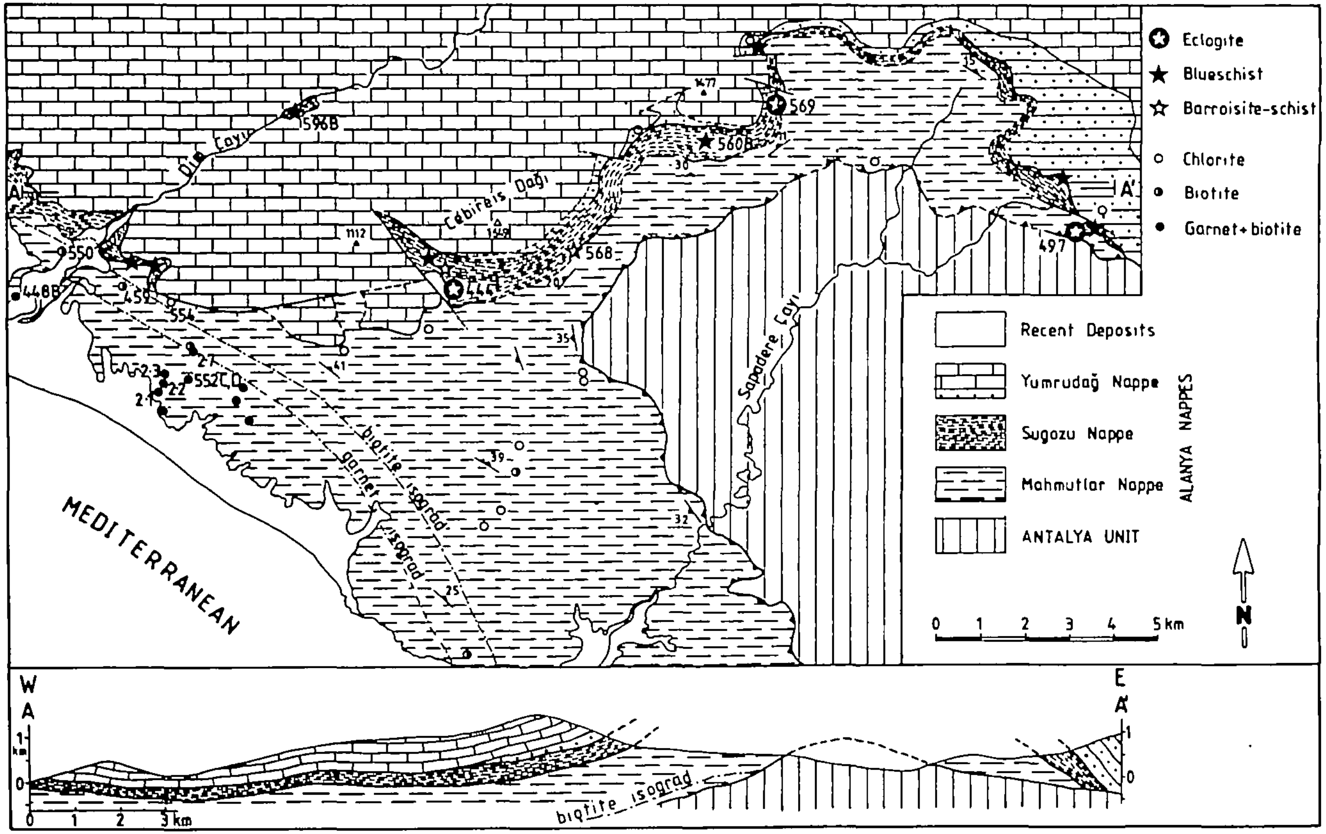

FIG. 2. Geological map and cross-section of the Alanya region with specimen locations. The various stars indicate the location of studied metabasic rock types in the Sugözü Nappe. The open, half-filled and filled circles indicate the location of the studied chlorite, biotite, and garnet zone assemblages of the Barrovian metamorphism. The sample numbers of the analysed specimens are also shown. Notice the absence of spatial relationship between the isograds in the Mahmutlar Nappe and paragenesis in the Sugözü Nappe.

ECLOGITE/BLUESCHIST FACIES METAMORPHISM

This early *HP/LT* metamorphism is documented only in the Sugözü Nappe, which is only 600 m thick but extends for over 40 km along the coast with a minimum width of 4 km (Fig. 2; Okay & Özgül, 1984). The Sugözü Nappe consists mainly of pelitic garnet–mica schists with the common mineral assemblage garnet + albite + chlorite + phengite + quartz (Table 1). These five minerals make up over 90% of the mode. Rutile, locally replaced by sphene, apatite, and tourmaline are accessory minerals. Small amounts of ilmenite, biotite, graphite, clinozoisite, and altered Fe-carbonate are present in many samples. Garnet and albite occur as rotated poikiloblasts up to 1 cm across surrounded by pale green chlorite, phengite, and quartz. The conspicuous garnet porphyroblasts in the mica schists were used in the field to map the boundaries of the Sugözü Nappe, as the overlying Yumrudağ Nappe and the directly underlying metasediments of the Mahmutlar Nappe lack garnet (Fig. 2). Garnets from the Sugözü Nappe commonly contain sigmoidal inclusion trails of quartz, clinozoisite, white mica, and rutile; rare sodic amphibole inclusions in the garnet prophyroblasts are the only evidence for *HP/LT* metamorphism in the garnet–mica schists.

Apart from the garnet–mica schists, the Sugözü Nappe also includes metaquartzite, metadolomite, and metabasite, which however make up less than 5% of the sequence. Metabasites occur within the garnet–mica schists as rare intercalated, conformable bands 0·2–0·3 m thick, or boudins up to 2 m across. They probably represent sills, dykes, or lava flows in a shale sequence.

Metabasites are variably affected by the later Barrovian metamorphism and can be classified into eclogites, blueschist–metabasites and barroisite–amphibolites (Fig. 2). The mineral assemblage in the eclogites is garnet + omphacite + glaucophane + paragonite + quartz + rutile + phengite (Table 1, Fig. 3A). Garnet occurs as idioblastic and frequently poikilitic porphyroblasts set in a parallel-aligned groundmass of elongate omphacite, glaucophane, white mica, and interstitial quartz (Fig. 3A). Garnet porphyroblasts are full of inclusions of quartz, clinozoisite, white mica, glaucophane, and rutile; commonly they have an inclusion-free outer rim. Omphacite forms pale green to colourless, subidioblastic elongate grains that are free of inclusions and are frequently rimmed by very fine-grained symplectitic intergrowths of albite and amphibole (Fig. 3A). Sodic amphibole occurs as pale blue to colourless idioblastic grains that occasionally have narrow rims of bluish-green barroisite. Eclogites grade into the blueschist metabasites with an increase in modal sodic amphibole, occasionally to the exclusion of sodic pyroxene (Table 1).

Analytical technique

The minerals in three specimens (426, 431, and 497B) were analysed by the energy dispersive electron microprobe system in the Department of Earth Sciences, University of Cambridge. All the other samples were analysed by a Cameca electron microprobe with automated wavelength-dispersive spectrometers in the Department of Earth and Space Sciences, UCLA. The mineral compositions were determined for at least ten elements (Na, Ca, K, Fe, Mg, Mn, Cr, Ti, Al, Si). The representative mineral compositions in Tables 2 and 4 are all point-analyses.

The method for estimating ferric ion in sodic pyroxene and in sodic amphibole is outlined in Okay (1978, 1980*a*). The Fe^{3+} in calcic and sub-calcic amphibole was estimated by assuming $Si + Ti + Al + Fe^{3+} + Fe^{2+} + Mg = 13{\cdot}00$, and a total ionic charge of 46.

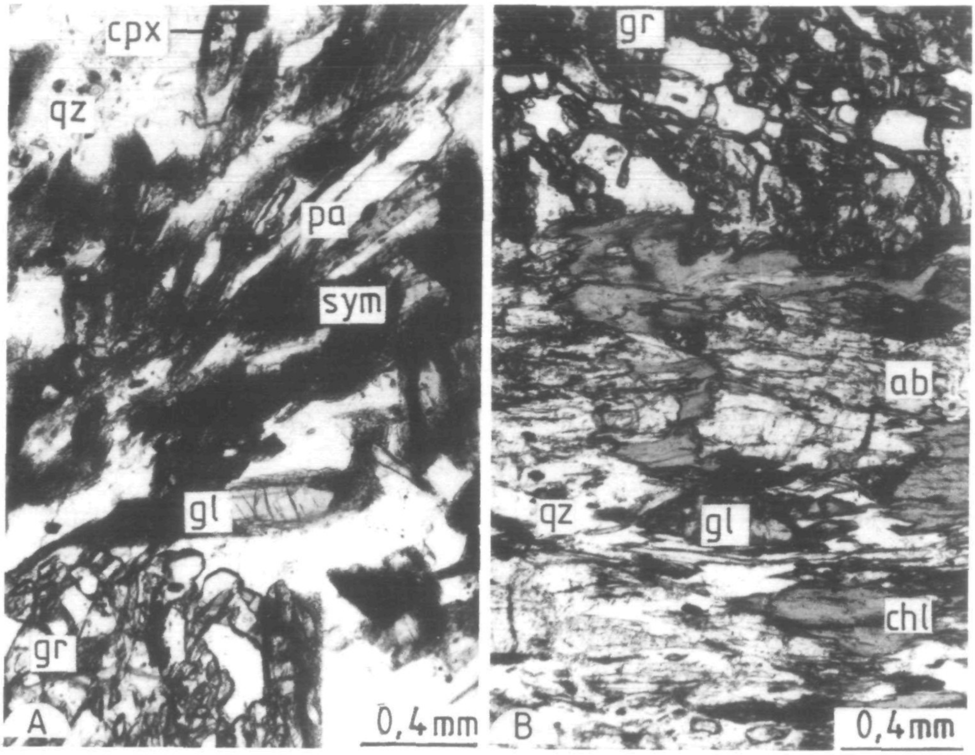

FIG. 3. Photomicrographs illustrating fluid-absent vs. fluid-present reaction products of the Sugözü eclogites along the same P–T path: (A) Quartz-eclogite (AL444) with the equilibrium assemblage of garnet (gr), omphacite (cpx), glaucophane (gl), paragonite (pa) and quartz (qz). Omphacite is partially broken down to a very fine-grained symplectite of albite and amphibole (sym). (B) Barroisite–amphibolite (AL596B) with garnet (gr), albite (ab), chlorite (chl), quartz (qz), white mica and resorbing glaucophane (gl).

Mineral chemistry

Minerals from seven metabasites and one garnet–mica schist were analysed by the electron microprobe (Table 1). Garnet compositions from these specimens are plotted in Fig. 4a in terms of pyrope, grossular, and almandine + spessartine end-members, and representative analyses are given in Table 3. Analysed garnets show complex but generally consistent zoning profiles. The important features of the zoning is a fluctuating increase in the almandine component towards the rim, which however, shows a sharp decrease in the inclusion-free outer rim of the garnet. Grossular component shows a fluctuating pattern while pyrope component and Mg/Fe ratio show a general smooth increase from core to rim.

Analysed sodic pyroxene compositions are plotted in the jadeite–acmite–augite ternary diagram in Fig. 5, and representative compositions are listed in Table 2. Sodic pyroxenes from two quartz-eclogites (444 and 569) are omphacites with acmite contents below 12%, while those from the eclogite 497B, where quartz occurs in minor amounts in the pressure shadows of garnets and is not in equilibrium with sodic pyroxene, are impure jadeites with high acmite contents. No zoning was detected in the omphacites.

Sodic amphibole from six analysed specimens shows a narrow compositional range and falls within the ferroglaucophane and glaucophane fields (Fig. 6, Table 2). An occasionally

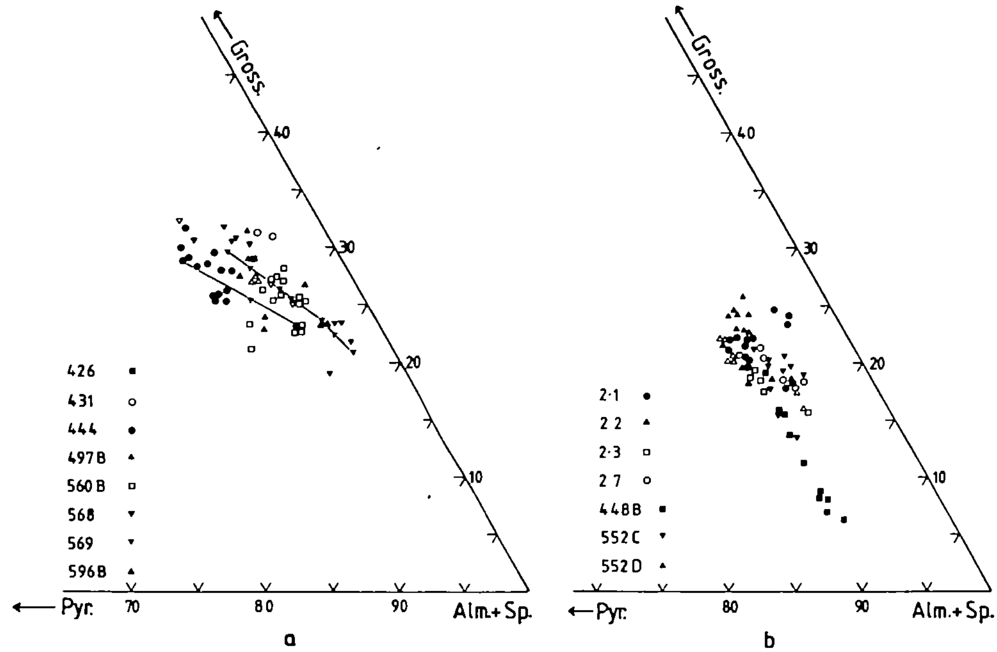

FIG. 4. (a) Garnet compositions from the HP/LT metabasites and micaschists of the Sugözü Nappe plotted on part of the pyrope–grossular–(almandine–spessartine) diagram in terms of mol%. Except for garnets from AL569, all spessartine contents are below 2·5%; lines join compositions from single grains. (b) Garnet compositions from the metapelites and metabasite of the Mahmutlar Nappe plotted on the same diagram.

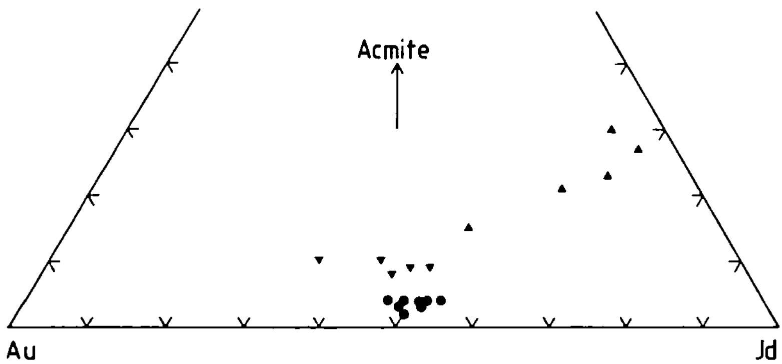

FIG. 5. Sodic pyroxene compositions from the Sugözü eclogites plotted on part of the acmite–jadeite–augite ternary diagram; symbols as in Fig. 4a.

observed discontinuous zoning in sodic amphibole involves an outward increase in Mg and Fe^{3+} at the expense of Fe^{2+} and Al (Fig. 6).

Although they are indistinguishable optically, paragonite and/or phengite occur in all analysed samples (Table 1). White mica compositions are plotted in Fig. 7 in terms of Si and Na/(Na+K) ratio, and representative compositions are given in Table 2. Paragonite compositions closely approximate the ideal formula with generally less than 15% muscovite substitution (Fig. 7); phengites show up to 10% paragonite and less than 2% margarite

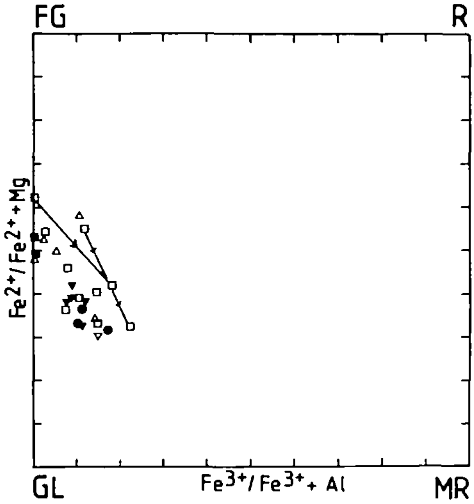

FIG. 6. Sodic amphibole compositions from the Sugözü metabasites. GL, glaucophane; FG, ferroglaucophane; R, riebeckite; MR, magnesioriebeckite. Symbols as in Fig. 4a.

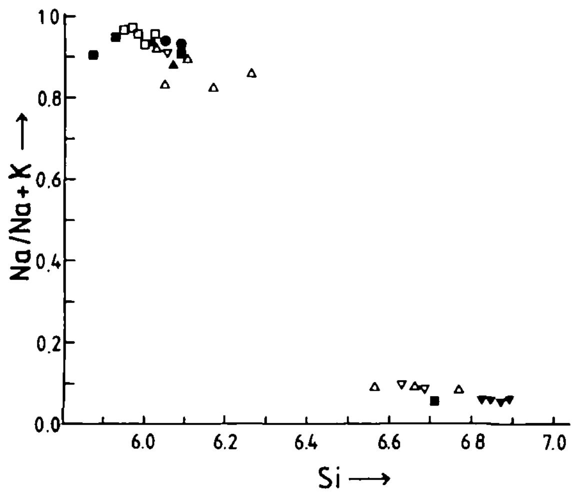

FIG. 7. Paragonite and phengite compositions from the metabasites and micaschist of the Sugözü Nappe. Symbols as in Fig. 4a.

substitution, and a variable Si content (Fig. 7). For a wide pressure range and at temperatures of above 400°C the paragonite–muscovite solvus indicates for coexisting micas $X_{Na}^{musc} \gg X_{K}^{parag}$ (Chatterjee & Flux, 1986). This is confirmed through the analysis of coexisting white micas from low to medium pressure metamorphic terrains (e.g., Thompson *et al.*, 1977; Droop, 1985). However, in the Sugözü eclogites and blueschists, the paragonite content of phengite is approximately equal to the muscovite content of the coexisting paragonite (Fig. 7, Table 2); a similar relation exists in the eclogites and blueschists of Sifnos (Schliestedt, 1986). This is due to the increased phengite substitution at high pressures which results in a symmetrical widening of the potassic white mica–paragonite solvus (cf. Chatterjee & Flux, 1986).

Clinozoisite is common as inclusions in garnet porphyroblasts but is not usually found in the matrix of the eclogites or blueschists (Table 1). Analysed clinozoisite inclusions have pistacite contents of 10–17%.

BARROVIAN METAMORPHISM

Yumrudağ Nappe

The Barrovian metamorphism increases in grade downward from the Yumrudağ to the Mahmutlar nappe. In the Yumrudağ Nappe, metabauxite lenses in the Permian carbonates contain corundum + diaspore + chloritoid + chlorite + kyanite + white mica (Peyronnet, 1971). In these rocks, diaspore is partly replaced by idiomorphic corundum crystals. The basal clastics of the Yumrudağ Nappe (Fig. 2) are generally completely reconstituted, and consist of quartz + white mica + chlorite + albite + calcite. However, large detrital microcline grains remain in many specimens. These incipiently metamorphosed clastics lie directly over the coarse-grained garnet–mica schists of the Sugözü Nappe.

Sugözü Nappe

In the Sugözü Nappe, Barrovian metamorphism was superimposed on an earlier *HP*/*LT* metamorphism. In the metabasite lithologies, the development of bluish-green barroisite rims around sodic amphibole, and the formation of abundant chlorite and albite are related to the later overprint. In the barroisite–amphibolites relict poikilitic garnet porphyroblasts are associated with abundant albite poikiloblasts with quartz inclusions, barroisite, chlorite, white mica, and quartz (Fig. 3B). Sphene replacing rutile, carbonate, clinozoisite, biotite, and pyrite occur in minor amounts in many samples (Table 1). In most barroisite–amphibolites, sodic amphibole is preserved in the cores of the hornblende grains.

Bluish-green amphibole compositions are shown in Fig. 8, and representative compositions are given in Table 2. They are barroisite in composition (Leake, 1978), and contain more Na and less Al^{IV} than the amphiboles from the Mahmutlar Nappe metabasites (Fig. 8). There is a major compositional break between sodic amphibole and barroisite (Fig. 8), which, however, cannot be interpreted as an immiscibility gap as the barroisite-forming reaction was most probably an irreversible non-equilibrium reaction.

Analysed albites from the barroisite–amphibolites contain a maximum of 3% anorthite component (Fig. 9). Chlorite, replacing garnet and locally sodic amphibole, shows a significant variation in Fe/(Fe + Mg) ratio even in a single probe section. Biotite occurs in very minor amounts ($<1\%$) in some barroisite–amphibolites and garnet–mica schists where it forms slender brown flakes in chlorite-rich patches.

Mahmutlar Nappe

Rocks of the Mahmutlar Nappe lie within the chlorite, biotite, and garnet zones of the Barrovian metamorphism (Fig. 2). Metapelites in the chlorite zone consist of white mica + quartz + albite + chlorite + ilmenite ± biotite. Biotite occurs sporadically in the chlorite zone, and makes up only a few modal percent, forming small brown flakes in the mica–chlorite matrix. Biotite becomes more abundant farther southwest, and it is possible to draw a biotite isograd in the field marking the first abundant and mesoscopically visible appearance of biotite (Fig. 2). Pelitic rocks in the biotite zone contain the assemblage quartz

TABLE 1

Measured modes of the analysed Sugözü Nappe rocks

		Eclogites	Blueschists		Barroisite-amphibolites			Micaschists	
	AL444	*AL569*	*AL497B*	*AL560B*	*AL596B*	*AL426*	*AL568*	*AL431*	*AL512*
Garnet	19·2	27·9	11·0	24·0	9·8	9·5	18·9	5·5	9·0
Omphacite	26·6(22·3)	32.8(21·5)	62·9	—	—	—	2·7(2·4)	—	—
Sodic amphibole	6·4(5·7)	2·7	3·5	22·4	8·1	10·7	3·4	0·2^{i}	—
White mica	8·8 p	3·9 m	15·0 p	1·8 p	11·3 p,m	8·9 p,m	3·8 p,m	18·8 m	19·2
Quartz	37·6	28·6	0·6	11·7	29·0	1·2	tr.	36·8	43·7
Rutile	1·0	0·2	3·2	1·3	0·3	0·1	1·6	tr.^{i}	tr.^{i}
Barroisite	tr.	tr.	—	0·2	1·8	17·8	44·4	—	—
Albite	—	—	—	7·5	25·2	23·1	16·6	22·5	25·0
Chlorite	—	—	0·5	24·2	12·5	9·6	2·6	9·4	1·9
Clinozoisite	tr.^{i}	0·1^{i}	0·1^{i}	0·3^{i}	0·3^{i}	0·2^{i}	1.1^{i}	tr.^{i}	tr.^{i}
Sphene	—	1.5	—	0·1	0·3	3·2	3·0	—	—
Calcite	—	1·3	—	—	—	3·2	—	—	—
Ankerite	—	—	—	—	—	9·3	—	—	0·2
Magnetite	—	—	1·6	—	—	—	—	—	—
Ilmenite	0·1	0·6	—	5·5	1·3	—	1·4	2·0	0·9
Pyrite	0·3	0·2	1·6	1·0	—	—	—	—	—
Biotite	—	—	—	—	—	1·7	0·5	4·6	tr.
Others		1,2		1	1,2	1,2,3	1	1,2	1

p, paragonite; m, phengite; tr < 0.1; i, inclusion in garnet; 1, apatite; 2, tourmaline; 3, pyrrhotite. The numbers in the brackets indicate the modal percent of albite + amphibole symplectite.

TABLE 2

Representative mineral compositions from the Sugözü Nappe

	Garnet				*Amphibole*				*Omphacite*		*Paragonite*		*Phengite*	
	AL444			*AL569*	*AL444*	*AL569*	*AL568*		*AL444*	*AL569*	*AL444*	*AL569*	*AL569*	*AL568*
	rim	*core*	*rim*	*rim*			*core*	*rim*						
SiO_2	38·77	38·53	39·05	38·45	58·25	57·59	57·32	49·95	56·88	56·18	47·46	48·15	50·26	50·82
TiO_2	0·08	0·09	0·09	0·10	0·12	0·01	0·05	0·28	0·02	0·04	0·07	0·08	0·28	0·32
Al_2O_3	21·88	21·42	21·57	21·25	11·62	11·78	12·35	11·40	12·36	11·88	39·46	40·20	25·88	29·95
FeO	26·44	30·67	27·10	28·26	10·18	11·16	10·21	12·79	4·26	5·35	0·30	0·54	2·15	2·33
MgO	2·91	1·77	3·06	1·87	9·61	9·04	9·96	11·62	7·46	6·82	0·16	0·14	3·33	3·16
MnO	0·11	1·01	0·11	0·36	0·02	0·11	0·03	0·10	0·07	0·10	0·00	0·01	0·00	0·02
CaO	10·58	8·24	10·31	10·99	0·53	0·43	1·39	7·69	12·04	11·54	0·19	0·15	0·03	0·01
Na_2O	0·00	0·00	0·00	0·00	7·48	7·23	7·01	3·90	7·87	8·31	6·64	6·23	0·45	0·69
K_2O	0·00	0·00	0·00	0·00	0·01	0·00	0·04	0·26	0·00	0·00	0·72	0·87	10·59	9·44
Total	100·77	101·73	101·29	101·28	97·82	97·35	98·36	97·99	100·91	100·22	95·00	96·37	92·97	96·74
						Ions on basis of								
	12 Oxygens				*23 Oxygens*				*4 cations*		*22 oxygens*		*22 oxygens*	
Si	3·02	3·02	3·03	3·01	7·94	7·94	7·78	7·08	1·99	1·98	6·06	6·05	6·88	6·64
Al^{IV}	0·00	0·00	0·00	0·00	0·06	0·06	0·22	0·92	0·01	0·02	1·94	1·95	1·12	1·36
Al^{VI}	2·01	1·98	1·97	1·96	1·81	1·85	1·76	0·99	0·50	0·47	3·99	4·01	3·06	3·25
Ti	0·01	0·01	0·01	0·01	0·01	0·00	0·01	0·03	0·00	0·00	0·01	0·01	0·03	0·03
Fe^{3+}	—	—	—	—	0·20	0·15	0·30	0·39	0·04	0·10				
Fe^{2+}	1·72	2·01	1·76	1·85	0·96	1·14	0·86	1·13	0·08	0·06	0·03	0·05	0·25	0·25
Mg	0·34	0·21	0·35	0·22	1·96	1·86	2·01	2·45	0·39	0·36	0·03	0·03	0·68	0·62
Mn	0·01	0·07	0·01	0·02	0·00	0·01	0·00	0·01	0·00	0·00	0·00	0·00	0·00	0·00
					4·94	5·01	4·94	5·00	1·01	0·99	4·06	4·10	4·02	4·15
Ca	0·88	0·69	0·86	0·92	0·08	0·06	0·20	1·18	0·45	0·44	0·03	0·02	0·00	0·00
Na	0·00	0·00	0·00	0·00	1·98	1·93	1·85	1·08	0·53	0·57	1·64	1·52	0·12	0·17
K	0·00	0·00	0·00	0·00	0·00	0·00	0·01	0·05	0·00	0·00	0·12	0·14	1·85	1·57
Total	7·98	7·99	7·99	7·99	15·00	15·00	15·00	15·31	3·99	4·00	13·85	13·79	13·99	13·89
Alm	58·3	67·5	59·1	61·5				Jd	50	46				
Spess	0·3	2·3	0·3	0·6				Ac	4	10				
Pyr	11·5	7·0	11·8	7·3				Au	46	44				
Gross	29·9	23·2	28·8	30·6										

Total iron as FeO.

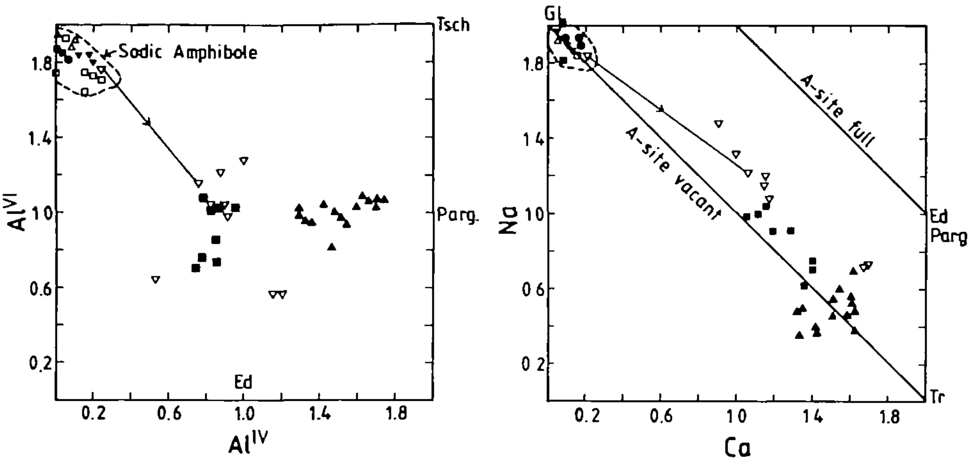

FIG. 8. Amphibole compositions from the Sugözü and Mahmutlar metabasites. Lines join compositions from single grains and arrows indicate the direction of the zoning. Symbols as in Fig. 4a except upward pointing filled triangles indicate amphibole compositions from the Mahmutlar metabasite AL552D.

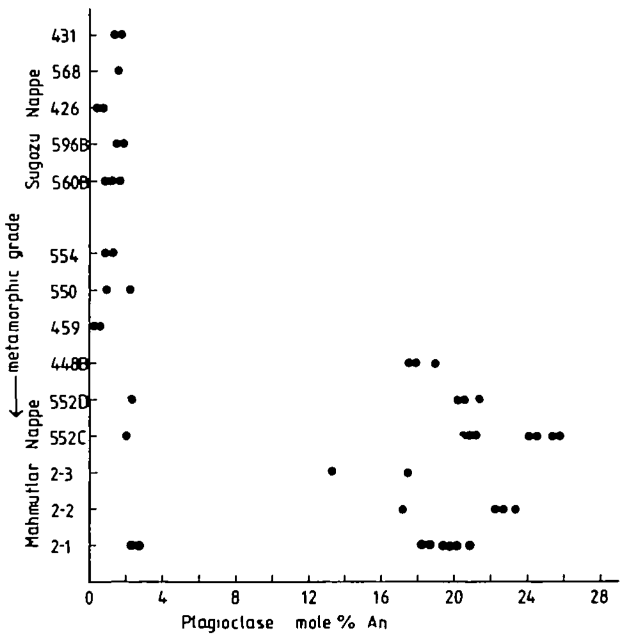

FIG. 9. Plagioclase compositions from the Sugözü and Mahmutlar Nappes. The specimen numbers are listed on the vertical axis in order of increasing Barrovian metamorphic grade.

+ albite + chlorite + white mica + biotite + ilmenite + graphite + calcite (Table 3). The garnet isograd, marking the first appearance of this phase in pelitic rocks, is relatively easy to delineate in the field. Metapelites in the garnet zone have the mineral assemblage of quartz + albite + oligoclase + chlorite + white mica + biotite + garnet + ilmenite + graphite (Table 3). Plagioclase and idioblastic garnet prophyroblasts are wrapped by a strongly parallel-aligned micaceous fabric of white mica, brown biotite, and pale-green chlorite with

TABLE 3

Mineral assemblages from the Mahmutlar Nappe

	Metapelites									Metabasite
	AL2-1	*AL2-2*	*AL2-3*	*AL552C*	*AL2-7*	*AL448B*	*AL459*	*AL550*	*AL554*	*AL552D*
Garnet	X	X	X	X	X	—	—	—	—	X
Biotite	X	X	X	X	X	X	X	X		X
White mica	X_m	$X_{m,p}$	X_m	$X_{m,p}$	X_m	—	X_m	X_m	X_m	$X_{m,p}$
Chlorite	X	X	X	X	X	X	X	X	X	X
Quartz	X	X	X	X	X	X	X	X	X	X
Plagioclase	X	X	X	X	—	X	X	X	X	X
Ilmenite	X	X	—	X	X	X	X	X	—	X
Calcic amphibole	—	—	—	—	—	—	—	—	—	X
Others						1				2

X_m, muscovite; $X_{m,p}$, muscovite and paragonite; 1, magnetite; 2, margarite.

interstitial quartz. Garnet and plagioclase porphyroblasts frequently have slightly rotated inclusions of quartz, graphite, and ilmenite.

Chlorite zone metabasites of the Mahmutlar Nappe largely retain the original igneous texture but consist of green actinolite + albite + epidote + sphene. Metabasites from the garnet zone (e.g., AL552D) contain hornblende + albite + oligoclase + garnet + biotite + white mica + chlorite + ilmenite. The absence of sodic amphibole in these metabasic rocks further indicates that the Mahmutlar Nappe has not shared the early *HP*/*LT* metamorphic history of the Sugözü Nappe.

Minerals from nine metapelites and one metabasite from the Mahmutlar Nappe, including one from the chlorite zone, two from the biotite zone, and seven from the garnet zone were analysed by the electron microprobe (Fig. 2). Garnet compositions from six metapelites and one metabasite are plotted in Fig. 4b in terms of pyrope, grossular, and almandine + spessartine end-members, and representative compositions are given in Table 4. These Barrovian garnets contain less grossular and pyrope, and more almandine components than garnets from the Sugözü eclogites and blueschists (Fig. 4b). However, this probably reflects lithological differences; garnets from the metabasite have similar compositions to those of the Sugözü eclogites and blueschists (Fig. 4b). Garnets from the Mahmutlar Nappe show simple zoning typical for garnets from metapelites; there is generally a smooth compositional variation, Mn and Ca decrease, and Fe and Mg increase from core to rim. This behaviour is typical for growth zoning produced as the garnet formed by a continuous reaction at the expense of the matrix minerals (Tracy *et al.*, 1976).

Several grains of biotite were analysed for each specimen. Mean biotite compositions are plotted in Fig. 10 and representative analyses are listed in Table 4. Biotites apparently show minor but regular decrease in Fe/(Fe + Mg) ratio with increasing grade although the variation in Fe/(Fe + Mg) ratio in biotites within a single probe section may be up to 10% (Fig. 10). Biotites from the metabasite are strongly alkali deficient probably due to partial chloritization, which might account for their rather low aluminium contents (Fig. 10).

Representative analyses of chlorite are also given in Table 4, and mean chlorite compositions from ten specimens are plotted in Fig. 10. There is generally a regular partitioning of Fe and Mg between biotite and chlorite (Fig. 10), and the partition coefficient of 0·95 $[(Fe/Mg)_{chl}/(Fe/Mg)_{bi}]$ is similar to those described from other Barrovian metamorphic terrains (e.g., Mather, 1970), and is higher than those from lower pressure metamorphic terrains (e.g., Ernst, 1983; Ferry, 1984). The Al/(Al + Fe + Mg) ratio of chlorites from the Mahmutlar Nappe (0·38–0·40) is significantly higher than the ratio from the glaucophane–lawsonite zone blueschists (0·29–0·36, Black, 1975; Okay, 1980*b*, Fig. 10) indicating that Si(Fe, Mg) substitutes for 2Al in chlorite with increasing pressure as in potassic white micas.

White mica in the metapelites occurs generally as parallel-aligned fibrous aggregates. Electron microprobe analyses reveal the presence of both muscovite and paragonite in many samples. Possibly due to the finely interlayered nature of the two micas, analyses indicate a spread of compositions between muscovite and paragonite, although at the temperatures of the garnet zone the muscovite–paragonite solvus should be wide (Flux & Chatterjee, 1986). Muscovite analyses in Table 4 are from metapelites where muscovite occurs as distinct individual flakes. Margarite occurs only in metabasite AL552D as fine-grained aggregates along with muscovite and paragonite.

Albite (An_{00-02}) is the only plagioclase in the biotite zone, whereas both albite (An_{02-03}) and oligoclase (An_{17-26}) occur in the garnet zone (Fig. 9). Albite and oligoclase occur as distinct grains and/or oligoclase forms sharp rims around albite crystals.

Amphibole from the metabasite AL552D is a tschermakitic hornblende (Leake, 1978)

Table 4

Representative mineral compositions from the Mahmutlar Nappe

	Garnet						Biotite				Muscovite			
	AL2-1		*AL2-3*	*AL552C*		*AL552D*	*AL2-1*	*AL2-3*	*AL552C*	*AL552D*	*AL2-1*	*AL2-3*	*AL552C*	*AL552D*
	core	*rim*	*rim*	*core*	*rim*	*rim*								
SiO_2	37·65	38·12	38·18	37·61	37·83	38·25	38·55	38·43	37·37	37·57	47·75	47·42	47·56	47·14
TiO_2	0·23	0·10	0·09	0·28	0·10	0·08	1·70	1·52	1·84	0·91	0·44	0·36	0·23	0·26
Al_2O_3	21·46	21·65	22·01	21·52	21·76	20·97	17·80	18·07	20·59	17·63	33·38	35·38	32·96	33·95
FeO	23·25	29·31	30·47	29·95	30·55	28·50	14·45	15·38	14·46	16·02	1·61	1·44	1·57	1·32
MgO	0·99	2·09	2·28	1·44	1·94	2·04	11·79	11·54	9·36	10·24	1·65	0·94	1·15	1·12
MnO	8·68	1·11	1·03	3·69	1·48	2·51	0·08	0·02	0·03	0·09	0·01	0·02	0·02	0·00
CaO	8·06	7·82	7·10	6·91	7·37	8·05	0·09	0·14	0·19	0·60	0·01	0·02	0·07	0·02
Na_2O	0·00	0·00	0·00	0·01	0·00	0·01	0·11	0·08	0·15	0·10	0·94	1·62	1·63	1·25
K_2O	0·00	0·00	0·01	0·00	0·00	0·00	8·56	7·75	8·10	4·83	9·44	8·41	7·65	9·10
Total	100·32	100·20	101·17	101·41	101·03	100·41	93·13	92·93	92·09	87·99	95·23	95·61	92·84	94·16
	Ions on basis of													
	12 oxygens						*22 oxygens*				*22 oxygens*			
Si	3·00	3·02	3·00	2·98	2·99	3·03	5·79	5·78	5·65	5·89	6·33	6·23	6·40	6·30
Al^{IV}	0·00	0·00	0·00	0·02	0·01	0·00	2·21	2·22	2·35	2·11	1·67	1·77	1·60	1·70
Al^{VI}	2·02	2·02	2·04	1·99	2·02	1·96	0·94	0·98	1·32	1·15	3·54	3·70	3·63	3·65
Ti	0·01	0·01	0·01	0·02	0·01	0·01	0·19	0·17	0·21	0·11	0·04	0·04	0·02	0·03
Fe	1·55	1·94	2·00	1·99	2·02	1·89	1·81	1·93	1·83	2·10	0·18	0·16	0·18	0·15
Mg	0·12	0·25	0·27	0·17	0·23	0·24	2·64	2·59	2·11	2·39	0·33	0·18	0·23	0·22
Mn	0·59	0·07	0·07	0·25	0·10	0·17	0·01	0·00	0·00	0·01	0·00	0·00	0·00	0·00
							5.59	5·67	5·47	5·76	4·09	4·08	4·06	4·05
Ca	0·69	0·66	0·60	0·59	0·62	0·68	0·02	0·02	0·03	0·10	0·00	0·00	0·01	0·00
Na	0·00	0·00	0·00	0·00	0·00	0·00	0·03	0·02	0·04	0·03	0·24	0·41	0·43	0·32
K	0·00	0·00	0·00	0·00	0·00	0·00	1·64	1·49	1·56	0·97	1·60	1·41	1·31	1·55
							1·69	1·53	1·63	1·10	1·84	1·82	1·75	1·87
Total	7·98	7·97	7·99	8·01	8·00	7·98	15·28	15·20	15·10	14·86	13·93	13·90	13·81	13·92
Alm	52·5	66·4	68·0	6·3	68·0	63·4								
Spess	20·0	2·4	2·4	8·3	3·4	5·7								
Pyr	4·1	8·6	9·2	5·7	7·7	8·1								
Gross	23·4	22·6	20·4	19·7	20·9	22·8								

TABLE 4 (*continued*)

	Plagioclase					Chlorite				Hornblende	Ilmenite	
	AL2-1	*AL2-3*	*AL552C*	*AL552D*		*AL2-1*	*AL2-3*	*AL552C*	*AL552D*	*AL552D*	*AL2-1*	*AL552C*
SiO_2	63·00	63·77	60·95	68·15	63·25	26·16	25·54	25·29	25·55	44·36	0·03	0·03
TiO_2	0·00	0·00	0·00	0·01	0·00	0·09	0·16	0·08	0·04	0·34	53·91	53·01
Al_2O_3	23·20	22·68	23·56	19·26	22·49	23·21	23·82	22·86	22·73	14·32	0·00	0·00
FeO	0·18	0·08	0·05	0·07	0·01	19·59	22·30	24·25	21·89	16·31	41·99	44·83
MgO	0·00	0·00	0·00	0·00	0·00	18·24	16·58	15·69	16·62	9·23	0·00	0·03
MnO	0·04	0·00	0·03	0·00	0·03	0·17	0·11	0·07	0·11	0·22	2·15	0·91
CaO	4·34	3·68	5·34	0·48	4·25	0·03	0·02	0·00	0·02	10·30	0·03	0·09
Na_2O	9·57	9·65	8·67	11·52	9·35	0·01	0·00	0·00	0·00	1·26	0·00	0·00
K_2O	0·12	0·06	0·05	0·06	0·11	0·09	0·03	0·01	0·02	0·32	0·00	0·03
Total	100·45	99·92	98·65	99·55	99·49	87·59	88·56	88·25	86·98	96·66	98·11	98·93
						Ions on basis of						
			8 oxygens					*28 oxygens*			*3 oxygens*	
Si	2·78	2·82	2·74	2·99	2·81	5·33	5·22	5·25	5·32	6·47	0·00	0·00
Al^{IV}	0·22	0·18	0·26	0·01	0·19	2·67	2·78	2·75	2·68	1·53	0·00	0·00
Al^{VI}	0·99	1·00	0·99	0·99	0·99	2·91	2·96	2·85	2·89	0·93	0·00	0·00
Ti	0·00	0·00	0·00	0·00	0·00	0·01	0·02	0·01	0·01	0·04	1·03	1·01
Fe^{3+}										0·87		
Fe^{2+}	0·01	0·00	0·00	0·00	0·00	3·34	3·81	4·21	3·81	1·12	0·89	0·95
Mg	0·00	0·00	0·00	0·00	0·00	5·54	5·05	4·86	5·15	2·01	0·00	0·00
Mn	0·00	0·00	0·00	0·00	0·00	0·03	0·02	0·01	0·02	0·03	0·05	0·02
Ca	0·20	0·17	0·26	0·02	0·20	0·01	0·00	0·00	0·00	1·64	0·00	0·00
Na	0·82	0·83	0·76	0·98	0·81	0·00	0·00	0·00	0·00	0·36	0·00	0·00
K	0·00	0·00	0·00	0·00	0·00	0·02	0·01	0·00	0·01	0·06	0·00	0·00
Total	5·02	5·00	5·01	4·99	5·00	19·86	19·87	19·94	19·89	15·06	1·97	1·98

Total iron as FeO.
Mineral compositions are used for geothermometry and geobarometry.

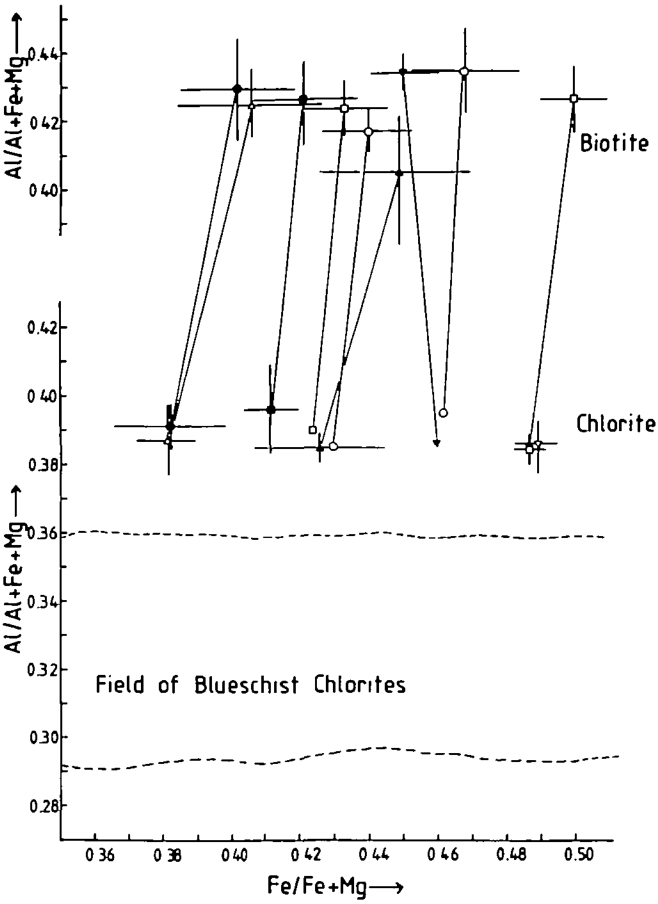

FIG. 10. Biotite and chlorite compositions from the Mahmutlar Nappe. The bars represent one standard deviation for analyses within one probe section. Lines join biotite and chlorite compositions from the same specimens. The compositional field of blueschist chlorites (Black, 1975; Okay, 1980) is also shown for comparison. Symbols as in Fig. 4b except filled squares and downward pointing open triangles indicate biotite and chlorite compositions from specimens AL459 and AL554 respectively.

characterized by little or no A-site occupancy and a relatively high Fe^{3+} content (Table 4, Fig. 8). Ilmenite is a ubiquitous accessory mineral and occurs in all analysed metapelites and in the metabasite. Analysed ilmenites closely approximate the ideal structural formula with only minor amounts of Mn (<3%) substituting for Fe.

PRESSURE AND TEMPERATURE CONDITIONS OF METAMORPHISM

Pressure and temperature of the eclogite metamorphism

The temperatures during the *HP*/*LT* metamorphism are estimated from the distribution of Fe^{2+} and Mg between garnet rims and omphacite using the Ellis & Green (1979) calibration. As there might have been re-equilibration during the Barrovian metamorphism, the compositions of the most pyrope-rich garnet rims and matrix omphacites were used. K_D values for omphacite–garnet from two of the least altered eclogites (AL444 and AL569, Table 1) range from 23 to 30, and indicate temperatures of 490–545 °C for the 10–15 kb pressure range (Fig. 11).

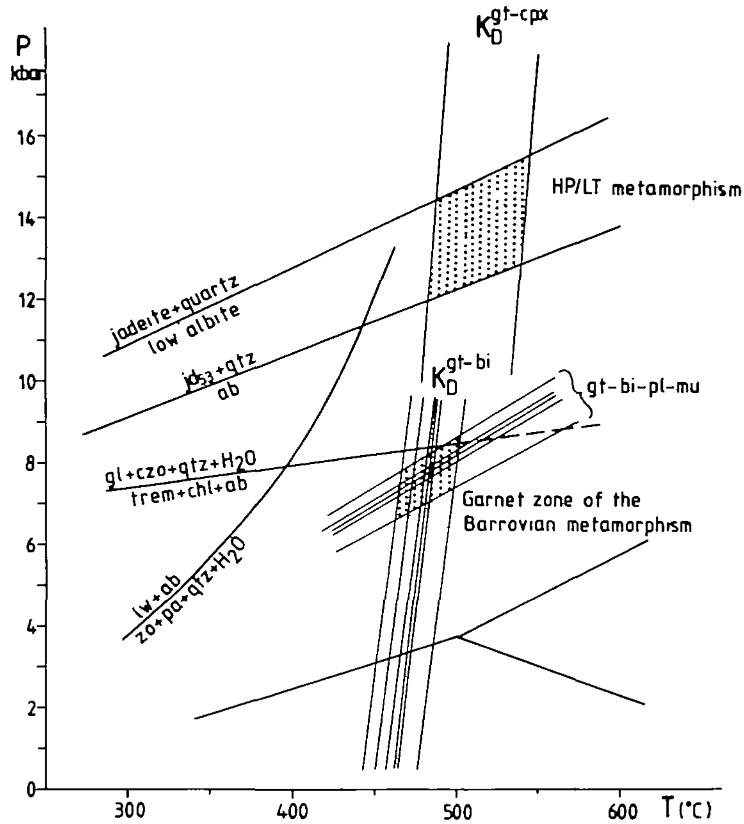

FIG. 11. Pressure–temperature diagram for the Alanya rocks displaying the peak metamorphic conditions of the eclogite facies metamorphism, and the garnet zone of the Barrovian metamorphism (stippled areas). The reaction lawsonite + albite = zoisite + paragonite + quartz + H_2O, and jadeite + quartz = low albite are calculated from the data of Holland & Powell (1985). The lower pressure breakdown reaction of glaucophane is after Maruyama *et al.* (1986). Also shown is the Al_2SiO_5 phase diagram after Holdaway (1971).

Although coexisting sodic and potassic white micas occur in the eclogites and blueschists of the Sugözü Nappe, the application of paragonite–muscovite geothermometry to these rocks is limited by the substantial deviation of the potassic white mica compositions from the muscovite–paragonite join (Fig. 7; Chatterjee & Flux, 1986) and by possible re-equilibration during the Barrovian metamorphism.

Metamorphic pressures were established from the reaction:

$$\underset{\text{albite}}{NaAlSi_3O_8} = \underset{\text{jadeite}}{NaAlSi_2O_6} + \underset{\text{quartz}}{SiO_2} \quad (1)$$

In the absence of albite in the eclogites, pyroxene is not saturated with respect to the jadeite content, and reaction (1) gives only a minimum pressure estimate. The low- to high-albite transition occurs above 640 °C (Goldsmith & Jenkins, 1985), so that a relatively ordered albite must have been the stable form during the H*P*/L*T* metamorphism. Using the thermodynamic data from Holland (1980) for low-albite and jadeite, and taking the activity of jadeite in omphacite equal to its mole fraction (cf. Holland, 1983), the highest analysed jadeite content in omphacite from the quartz-eclogite ($X_{Jd} = 0{\cdot}53$ in AL444) yields a minimum pressure estimate of 12·5 kb for the temperature range of interest.

Albite is a major phase in the garnet–mica schists, usually making up more than 20% of the mode (Table 1); there are no indications that jadeite was originally present in these garnet–mica schists. Furthermore, although albite inclusions are occasionally present in the garnet porphyroblasts of the garnet–mica schists, no jadeite inclusions or radial cracks around albite inclusions were detected, suggesting that albite was stable during the H*P*/L*T* metamorphism. Therefore reaction (1) also provides an upper pressure limit of 15 kb for the H*P*/L*T* metamorphism (Fig. 11).

Summarizing the data presented, rocks of the Sugözü Nappe were initially crystallized at peak temperatures of 510 ± 25 °C and at pressures of $13{\cdot}5 \pm 1{\cdot}5$ kb. These temperatures and pressures of recrystallization are similar to the conditions of metamorphism of other Group C eclogites (cf. Newton, 1986).

Pressure and temperature in the garnet zone of the Barrovian metamorphism

The temperature of recrystallization in the garnet zone of the Barrovian metamorphism was estimated using garnet/biotite geothermometry. The Ferry & Spear (1978) calibration as modified by Hodges & Spear (1982) was used, which corrects for the grossular component in garnet, and appears to give the best results in this medium grade (cf. Ashworth & Evirgen, 1985*a*). Twenty-one adjoining garnet/biotite pairs from six garnet zone metapelites (Table 3) indicate a mean temperature of 469 °C with one standard deviation of 13 °C at 6·5 kb (Fig. 11). The direct application of the Ferry & Spear (1978) calibration gives the unrealistically low temperature of 406 ± 18 °C. The garnet zone metabasite AL552D gives a temperature of 540 °C by the garnet/biotite geothermometer of Hodges & Spear (1982), and 545 °C by the garnet/hornblende geothermometer of Graham & Powell (1984). These rather high temperatures are most likely due to the high Fe^{3+} content of amphibole and partial chloritization of the biotite from the metabasite (Table 4). The metamorphic temperature drops to 467 °C when the recalculated Fe^{2+}/Mg rather than the Fe/Mg ratio in amphibole is used for the garnet/hornblende geothermometry.

Pressures of Barrovian metamorphism in the garnet zone were estimated using the garnet–biotite–plagioclase–muscovite geobarometry of Ghent & Stout (1981), and Hodges & Crowley (1985). Pressures were calculated for nine coexisting garnet (Alm_{64-70} $Gross_{18-23}$ Pyr_{8-10} $Spess_{2-6}$)–plagioclase (An_{17-25})–biotite–muscovite subassemblages from five samples (Table 4). A subassemblage was defined when all four minerals occurred within an area of about 2 mm^2. In specimens where white mica analyses gave a range of $K/(K+Na)$ ratios, muscovite compositions with the highest $K/(K+Na)$ ratio in the subassemblage were used in the geobarometric calculations. The Hodges & Crowley (1985) calibration gave a mean pressure of 7·6 kb with one standard deviation of 0·4 kb at 469 °C, whereas the Ghent & Stout (1981) calibration indicated a pressure of 7·5–8·5 kb at the same temperature. The computed constant K_D lines based on the Hodges & Crowley (1985) method are shown in Fig. 11.

The major uncertainty in the garnet–biotite–plagioclase–muscovite geobarometer is the anorthite activity in the albite-rich plagioclase. Ghent & Stout (1981) did not specify individual activity coefficients; instead they used a temperature-dependent empirical constant for the activity coefficients of all the four minerals. Hodges & Crowley (1985) assumed a purely temperature-dependent activity coefficient for anorthite in plagioclase (cf. Orville, 1972), which gives $\gamma_{An} = 1{\cdot}55$ at 469 °C. The Al-avoidance model of Kerrick & Darken (1975) as applied by Newton *et al.* (1980) indicates higher activity coefficients for anorthite of about 1·9–2·1 for An_{17} to An_{25} at 469 °C. These higher activity coefficients for anorthite reduce the calculated pressures by about 0·8–0·9 kb. Based on a comparison of plagioclase-free and plagioclase-bearing geobarometers, Ashworth & Evirgen (1985*b*) suggest that, for plagioclase compositions around the peristerite gap (An_{14-22}), the activity coefficient of anorthite is grossly underestimated by both of these models, and they put forward an empirical activity-composition relation for plagioclase of this anorthite range, which involves activity coefficients as high as 7 for An_{14}. Using these activity coefficients, the calculated pressures for the garnet zone assemblages of the Mahmutlar Nappe are reduced to about 5·5 kb.

In the face of these disparate pressure estimates, comparison with the garnet zone assemblages from other terrains is instructive. Garnet zone metapelites from the southwest Tauern Window in the Eastern Alps, described by Selverstone & Spear (1985), were metamorphosed at nearly the same temperatures (474 ± 25 °C) as the garnet zone metapelites from the Mahmutlar Nappe (469 ± 13 °C). Although garnet, biotite, and muscovite compositions are similar in both areas, coexisting plagioclase from the southwest Tauern Window is much more anorthite-rich (An_{43-50}) than the equivalent plagioclase from the Mahmutlar Nappe (An_{17-25}), indicating that pressures were lower in the southwest Tauern Window. Metamorphic pressures in the southwest Tauern Window calculated using the garnet–biotite–plagioclase–muscovite geobarometer of Hodges & Crowley (1985) come out to be 5·5 kb (Selverstone & Spear, 1985). The anorthite activity of 1·55 used in this geobarometric calculation is a reasonable and safe estimate for this anorthite range (An_{43-50}), thus indicating that the pressures in the garnet zone of the Mahmutlar Nappe were higher than 5·5 kb. An average pressure of 6·5 kb is accepted for the garnet zone assemblages from the Mahmutlar Nappe, which best conforms with the anorthite activity model of Newton *et al.* (1980). Amphibole compositions from the garnet zone metabasite of the Mahmutlar Nappe plot within the medium- and high-pressure amphibole fields defined by Laird & Albee (1981*b*), attesting to the relatively high pressures during the Barrovian metamorphism.

In conclusion, the garnet zone rocks of the Mahmutlar Nappe were equilibrated at peak temperatures of 469 ± 13 °C and at pressures of 6·5 ± 1·0 kb.

METAMORPHIC REACTIONS AND *P–T* PATHS

Sugözü Nappe

The earliest preserved mineral assemblage in the Sugözü Nappe is the eclogite assemblage estimated to have formed at 510 ± 25 °C and 13·5 ± 1·5 kb (Fig. 11). The essential eclogite assemblage of garnet + omphacite + glaucophane + paragonite in the Sugözü Nappe lies, in the quartz-bearing rocks, in the six component system of Na_2O–CaO–FeO–MgO–Al_2O_3–H_2O. Fe_2O_3 occurs in minor amounts both in omphacite and sodic amphibole, and can be neglected to a first approximation. Phase relations in the eclogite can be illustrated in a Na–Ca–Fe^{2+}, Mg (NCF) ternary diagram (Fig. 12) by projecting from paragonite and assuming a fixed a_{H_2O}. The NCF diagram in Fig. 12 shows the incompatibility of glaucophane and clinozoisite in the eclogite facies in the model system. Clinozoisite is generally absent in the matrix of the Sugözü eclogites (Table 1), although it is very common as an inclusion phase in the garnets. This suggests that the eclogite assemblage of omphacite and garnet was formed by a reaction:

$$1{\cdot}45\ \text{glaucophane} + 1{\cdot}36\ \text{clinozoisite} = \text{garnet} + 0{\cdot}34\ \text{paragonite} + 4{\cdot}28\ \text{omphacite} + 2{\cdot}10\ \text{quartz} + 1{\cdot}43\ H_2O. \qquad (2)$$

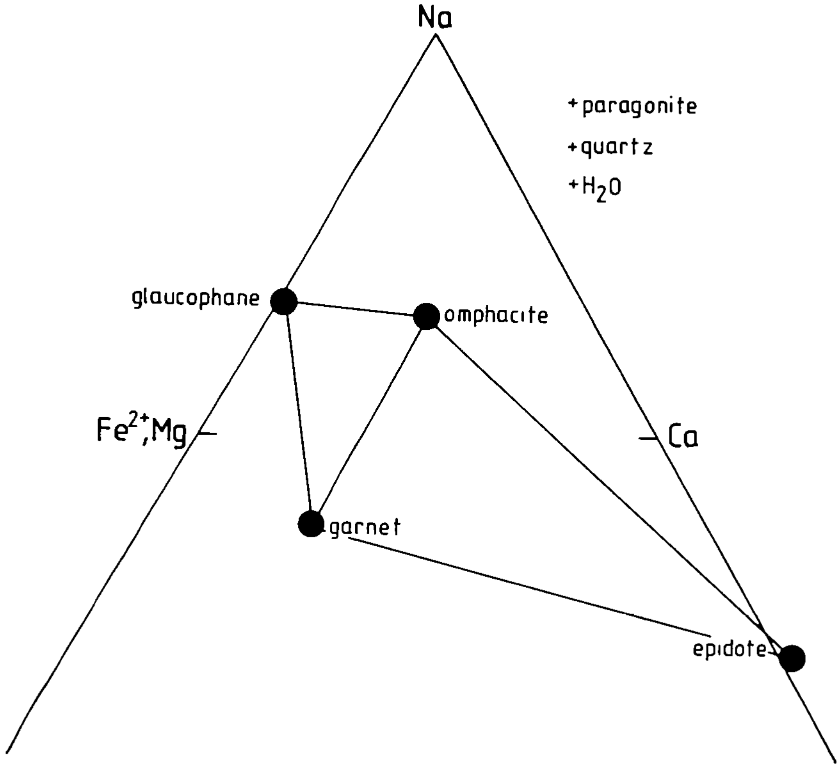

FIG. 12. Projection of mineral compositions of the quartz-eclogite AL444 from paragonite, quartz, and H_2O onto the Na–Ca–Fe, Mg plane, illustrating the phase relations in blueschist eclogites.

A similar eclogite-forming reaction was deduced by Ridley (1984) in the H*P*/L*T* metamorphic rocks of Syros in the Cyclades. Reaction (2) is balanced in the six component system (Na–Ca–Fe^{2+}, Mg–Al–Si–H) for the analysed mineral compositions from the eclogite AL444 and using an average clinozoisite composition from the garnet cores (cf. Table 2). However, due to the unequal partitioning of Fe^{2+} and Mg between the phases, reaction (2) will be a continuous reaction, and all the phases in reaction (2) can coexist as an equilibrium assemblage over a range of pressure and temperature, as reported in eclogites from Sifnos, Cyclades (Schliestedt, 1986). Under transition conditions, rocks with high Fe^{3+}/Al and Mg/Fe^{2+} ratios will develop blueschist as opposed to eclogite mineral assemblages (cf. Brown & Bradshaw, 1979).

In the Sugözü eclogites, reaction (2) was terminated by the complete consumption of clinozoisite in the matrix. Ridley (1984) estimates reaction (2) to be nearly isothermal so that the formation of the eclogite assemblage will be favoured by increasing temperature and/or decreasing a_{H_2O}. In the Sugözü garnets, the increasing Mg/Fe ratio from core to rim suggests that reaction (2) was due to the rising temperature. This, together with the absence of jadeite in the garnet–mica schists puts close constraints on the prograde *P*–*T* path of the Sugözü rocks (Fig. 13).

The next reaction recorded in the metabasic rocks of the Sugözü Nappe is the development of the greenschist mineral assemblages of the Barrovian metamorphism. This reaction was clearly controlled by the supply of H_2O-rich fluids; eclogites, which have remained dry have only developed thin nebulous coronas around omphacite or sodic

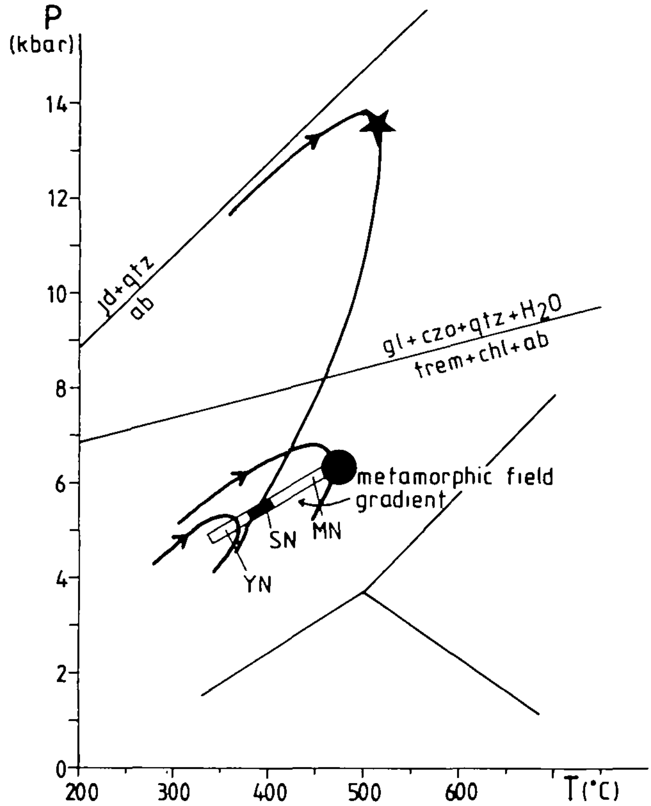

FIG. 13. Probable P–T paths for the Alanya Nappes. The star and the filled circle indicate the estimated P–T conditions of the eclogite facies metamorphism and of the garnet zone of the Barrovian metamorphism respectively. A possible metamorphic field gradient for the Barrovian metamorphism is also shown with the respective location of the Alanya Nappes, MN, Mahmutlar Nappe; SN, Sugözü Nappe, YN, Yumrudağ Nappe. The other reaction curves are as in Fig. 11.

amphibole (Fig. 3A), typical for reactions involving no fluid phase. This suggests that after the climax of the HP/LT metamorphism, the fluid phase was expelled from the Sugözü rocks.

The development of the greenschist facies mineral assemblages in the eclogites and blueschists can be described by the reaction:

$$\text{glaucophane} + \text{omphacite} + \text{garnet} + H_2O = \text{albite} + \text{chlorite} + \text{barroisite}. \quad (3)$$

In the Sugözü rocks, reaction (3) was an irreversible disequilibrium reaction in that the eclogite/blueschist mineral assemblages were not stable around the P–T conditions of reaction (3). The abrupt and prolific development of chlorite and albite in some metabasic rocks (Table 1) indicates that the metastable eclogite/blueschist mineral assemblages were rapidly overprinted once fluid entered the rock; only garnet survived as a metastable phase.

An independent upper pressure estimate for the Barrovian metamorphism in the Sugözü Nappe is given by the experimentally determined lower pressure stability of sodic amphibole through the reaction of (Fig. 11; Maruyama *et al.*, 1986):

$$\text{sodic amphibole} + \text{clinozoisite} + \text{quartz} + H_2O = \text{albite} + \text{tremolite} + \text{chlorite}. \quad (4)$$

The sodic amphibole used by Maruyama *et al.* (1986) in the experimental work is compositionally similar to the sodic amphiboles from the Sugözü Nappe, so that their results are applicable. Reaction (4) has a shallow slope in the *P–T* coordinates and occurs at a pressure of around 8 kb in the 350–450 °C temperature range (Fig. 11). This is compatible with the pressures of 6·5 kb for the Barrovian metamorphism estimated from the garnet zone assemblages. The temperature of the Barrovian metamorphism in the Sugözü Nappe is constrained below 460 °C by the location of the Sugözü Nappe on the low-temperature side of the garnet isograd (Fig. 2) and above 350 °C by the absence of lawsonite in the mineral assemblage (Fig. 11); a further upper temperature limit is given by the typical biotite zone temperatures of 410–440 °C (Laird & Albee, 1981*b*; Ferry, 1984).

The narrow age span between the *HP*/*LT* and Barrovian metamorphism (M. Satır, pers. comm.) and the tectonic features of the Sugözü Nappe make the uplift of the Sugözü rocks to the surface and their reburial quite unlikely. The nappe contacts in the Alanya area are subparallel to the penetrative cleavage in the rocks defined by the mica grains of the Barrovian metamorphism. This, together with the continuity of the Barrovian metamorphism across the nappe boundaries suggest that the Barrovian metamorphism and associated deformation were contemporaneous with the stacking of the Alanya Nappes.

Thus, Sugözü rocks which were initially recrystallized at about 13·5 kb and 510 °C, remained dry and unreactive on their uplift and cooling path until they were juxtaposed with the Mahmutlar and Yumrudağ Nappes at pressures of around 6 kb and temperatures of 400 °C (Fig. 13). H_2O-rich fluids, probably derived from the dehydration reactions in the Mahmutlar Nappe triggered local metamorphic reactions, such as reaction (3), in the eclogites of the Sugözü Nappe. A similar fluid induced greenschist facies metamorphic overprint on eclogites and blueschists is described from the Cycladic island Sifnos in Greece (Matthews & Schliestedt, 1984; Schliestedt & Matthews, 1987).

One important and interesting feature of the *P–T* uplift path of the Sugözü Nappe is that the eclogites underwent a cooling of around 100 °C during decompression from 13·5 to 6 kb (Fig. 13), whereas the *P–T* paths of most high-pressure rocks are considered to involve heating during decompression (e.g., Holland & Richardson, 1979). Thermotectonic models of metamorphism also indicate heating during decompression for most boundary conditions (England & Thompson, 1984). However, the temperature conditions of the Barrovian overprint on blueschists and eclogites are difficult to establish with any accuracy in the absence of independent *P–T* evidence such as in the Alanya area (e.g., Ernst, 1976), and cooling during decompression of the eclogites could be more widespread than hitherto recognized. Another example of cooling during uplift of the eclogites comes from Sifnos, Greece, where oxygen isotope geothermometry indicates lower temperatures for the greenschist facies overprint compared to that of the initial *HP*/*LT* metamorphism (Matthews & Schliestedt, 1984).

Mahmutlar and Yumrudağ Nappes

A probable metamorphic field gradient (Spear *et al.*, 1984) for the Barrovian metamorphism in the Alanya area is shown in Fig. 13. This is mainly based on the estimated *P–T* conditions of the garnet zone. As the structural thickness of the Alanya Nappes in the studied area is less than 4 km, and as the studied area is relatively small (Fig. 2), the pressure during the Barrovian metamorphism did not vary significantly across the investigated area even if the isobars were oblique to the nappe boundaries. The garnet isograd, regarded as close to an isotherm, is subparallel with the nappe boundaries (Fig. 2), indicating that the temperature decreased upwards in the structural sequence during the Barrovian metamorphism. A temperature of about 350 °C, based on the absence of lawsonite in the Yumrudağ and Sugözü Nappes, is taken as the lower temperature limit of the Barrovian metamorphism in the Alanya area (Fig. 13). The presence of corundum and kyanite in the metabauxites of the Yumrudağ Nappe is most probably due to reduced X_{H_2O} during the metamorphism of the carbonates.

The absence of sodic amphibole in the chlorite to garnet zone metabasites of the Mahmutlar Nappe indicates that the recrystallization occurred under increasing but not high pressure conditions. The garnet zoning profiles from the Mahmutlar Nappe, which show an increase in Mg/Fe ratio towards the rim, also suggests that the temperature was rising during growth of the garnets (Tracy *et al.*, 1976). There is little independent evidence for the shape of the *P–T* path for the Yumrudağ Nappe made up dominantly of carbonates. However, its very low-grade metamorphism and the absence of lawsonite put close constraints on the possible *P–T* paths for the Yumrudağ Nappe rocks.

Thus, unlike the Sugözü Nappe, rocks from the Mahmutlar and probably from the Yumrudağ Nappe were recrystallized during Barrovian metamorphism under increasing pressure and temperature conditions. The *P–T* paths of the Yumrudağ and Mahmutlar Nappes are shown in Fig. 13 as clockwise loops, which seem to be the most common *P–T* paths in metamorphic terrains from orogenic belts such as the Taurides (e.g., England & Thompson, 1984).

CONCLUSIONS

The Alanya area illustrates the possibility that large exotic H*P*/L*T* metamorphic slices could be present in Barrovian metamorphic terrains. Such slices could be difficult to recognize especially if the metamorphic overprint is strong. Thus, the presence of relict blueschist assemblages in Barrovian metamorphic belts does not necessarily imply that the whole metamorphic belt has undergone an early H*P*/L*T* metamorphism. Another example of such an exotic metamorphic slice is the 'eclogite zone' in the Tauern Window (Miller, 1974; Holland, 1979). However, in the Tauern Window, the whole nappe stack including the eclogite zone has undergone a blueschist facies metamorphism prior to the Barrovian metamorphism.

The Barrovian overprint on the eclogite mineral assemblages observed in the Alanya area was clearly not due to slow, passive uplift and resultant thermal relaxation as implied by thermotectonic models of metamorphism, or buoyant upward adiabatic decompression of a high-pressure unit. In fact, the Barrovian overprint occurred at lower temperatures than that of the initial eclogite metamorphism, and was due to tectonic juxtaposition of the nappes. Furthermore, the extent of the Barrovian overprint was strongly controlled by the availability of fluid (cf. Schliestedt & Matthews, 1987). Eclogites, which have remained dry only show symplectitic reaction rims (Fig. 3A) characteristic of fluid-absent reactions. Thus, Sugözü eclogites on their uplift path recorded *P–T* conditions along which fluids had access to the rocks. As the uplift path of most H*P*/L*T* metamorphic complexes passes through the field of Barrovian metamorphism, the Barrovian overprint observed in many H*P*/L*T* metamorphic terrains e.g., in the Alps (Frey *et al.*, 1974; Ernst & Dal Piaz, 1978), could simply be due to the availability of H_2O during this part of the uplift *P–T* section, and not necessarily due to increased temperature caused by slow uplift.

The tectonic setting, the thin and rootless nappe feature of the Sugözü rocks, and the absence of major clastic deposits of Late Cretaceous–Paleocene age in the Central Taurides precludes block uplift of the Sugözü rocks through erosion. The cooling involved during uplift implies rapid upward movement, probably in a subduction zone. The Sugözü rocks probably slid rapidly upwards as a thin sheet along a subduction zone with the shale-type lithologies providing both buoyancy and lubrication. The upward movement of the Sugözü rocks was arrested at a depth of about 23 km when they were interleaved and welded with the rocks of the Mahmutlar and Yumrudağ Nappes.

ACKNOWLEDGEMENTS

The project was supported by a TÜBİTAK post-doctoral research grant and NSF grant EAR 83-12702 to W. G. Ernst; the field support was provided by the Mineral Research and Exploration Institute of Turkey. R. E. Jones is thanked for assistance with the electron microprobe, and N. Özgül for help during the field work. This paper was critically reviewed and improved by W. G. Ernst, B. W. Evans, A. M. C. Sengör, and by an anonymous reviewer.

REFERENCES

Ashworth, J. R., & Evirgen, M., 1985*a*. Plagioclase relations in pelites, central Menderes Massif, Turkey. I. The peristerite gap with coexisting kyanite. *J. metamorphic Geol.* **3**, 207–18.

——— 1985*b*. Plagioclase relations in pelites, central Menderes Massif, Turkey. II. Perturbation of garnet-plagioclase geobarometers. *Ibid.* **3**, 219–30.

Black, P. M., 1975. Mineralogy of New Caledonian metamorphic rocks. IV. Sheet silicates from the Ouegoa District. *Contr. Miner. Petrol.* **49**, 269–84.

Blumenthal, M. M., 1951. Researches géologiques dans le Taurus occidental dans l'arrière-pays d'Alanya. *Publ. Miner. Res. Explor. Inst. Turkey*, D5, 134 pp.

Brown, E. H., & Bradshaw, J. Y., 1979. Phase relations of pyroxene and amphibole in greenstone, blueschist and eclogite of the Franciscan Complex, California. *Contr. Miner. Petrol.* **71**, 67–83.

Brunn, J. H., Dumont, J. F., Graciansky, P. C., Gutnic, M., Juteau, T., Marcoux, J., Monod, O., & Poisson, A., 1971. Outline of the geology of the western Taurids. In: Campbell, A. S. (ed.) *Geology and History of Turkey*. Petrol. Expl. Soc. Libya, 225–55.

Chatterjee, N. D., & Flux, S., 1986. Thermodynamic mixing properties of muscovite–paragonite crystalline solutions at high temperatures and pressures and their geological applications. *J. Petrology* **27**, 677–93.

Droop, G. T. R., 1985. Alpine metamorphism in the south-east Tauern Window, Austria: 1. *P–T* variations in space and time. *J. metamorphic Geol.* **4**, 371–402.

Ellis, D. J., & Green, D. H., 1979. An experimental study of the effect of Ca upon garnet–clinopyroxene Fe–Mg exchange equilibria. *Contr. Miner. Petrol.* **71**, 13–22.

England, P. C., & Richardson, S. W., 1977. The influence of erosion upon the mineral facies of rocks from different metamorphic environments. *J. geol. Soc. Lond.* **134**, 201–13.

—— Thompson, A. B., 1984. Pressure–temperature–time paths of regional metamorphism. I. Heat transfer during the evolution of regions of thickened continental crust. *J. Petrology* **25**, 894–928.

Ernst, W. G., 1976. Mineral chemistry of eclogites and related rocks from the Voltri Group, western Liguria, Italy. *Schweiz. Miner. Petrogr. Mitt.* **56**, 293–343.

—— 1983. Mineral parageneses in metamorphic rocks exposed along Tailuko Gorge, Central Mountain Range, Taiwan. *J. metamorphic Geol.* **1**, 305–30.

—— Dal Piaz, G. V., 1978. Mineral parageneses of eclogitic rocks and related mafic schists of the Piemonte ophiolite nappe, Breuil–St. Jacques area, Italian Western Alps. *Am. Miner.* **63**, 621–40.

Ferry, J. M., 1984. A biotite isograd in south-central Maine, USA: Mineral reactions, fluid transfer and heat transfer. *J. Petrology* **25**, 871–93.

—— Spear, F. S., 1978. Experimental calibration of the partitioning of Fe and Mg between biotite and garnet. *Contr. Miner. Petrol.* **66**, 113–7.

Flux, S., & Chatterjee, N. D., 1986. Experimental reversal of the reaction between muscovite–paragonite crystalline solutions and a 2 molal aqueous (Na, K)Cl fluid. *J. Petrology* **27**, 665–76.

Frey, M., Hunziker, J. C., Frank, W., Bocquet, J., Dal Piaz, G. V., Jager, E., & Niggli, E., 1974. Alpine metamorphism of the Alps, a review. *Schweiz. Miner. Petrogr. Mitt.* **54**, 247–90.

Ghent, E. D., & Stout, M. Z., 1981. Geobarometry and geothermometry of plagioclase–biotite–garnet–muscovite assemblages. *Contr. Miner. Petrol.* **76**, 92–7.

Goldsmith, J. R., & Jenkins, D. M., 1985. The high-low albite relations revealed by reversal of degree of order at high pressures. *Am. Miner.* **70**, 911–23.

Graham, C. M., & Powell, R., 1984. A garnet–hornblende geothermometer: calibration, testing and application to the Pelona Schist, southern California *J metamorphic Geol.* **2**, 13–32.

Gray, J. R., & Yardley, B. W. D., 1979. A Caledonian blueschist from the Irish Dalradian. *Nature* **278**, 736–7.

Hodges, K. V., & Crowley, P., 1985. Error estimation and empirical geothermobarometry for pelitic systems. *Am. Miner.* **70**, 702–9.

—— Spear, F. S., 1982. Geothermometry, geobarometry and the Al_2SiO_5 triple point at Mt. Moosilauke, New Hampshire. *Ibid.* **67**, 1118–34.

Holdaway, M. J., 1971. Stability of andalusite and the aluminium silicate phase diagram. *Am. J. Sci.* **271**, 97–131.

Holland, T. J. B., 1979. High water activities in the generation of high pressure kyanite eclogites of the Tauern Window, Austria. *J. Geol.* **87**, 1–29.

—— 1980. The reaction albite = jadeite + quartz determined experimentally in the range 600–1200 °C. *Am. Miner.* **65**, 129–34.

—— 1983. The experimental determination of activities in disordered and short-range ordered jadeitic pyroxenes. *Contr. Miner. Petrol.* **82**, 214–20.

—— Powell, R., 1985. An internally consistent thermodynamic dataset with uncertainties and correlations. 2. Data and results. *J. metamorphic Geol.* **3**, 343–70.

—— Richardson, S. W., 1979. Amphibole zonation in metabasites as a guide to the evolution of metamorphic conditions. *Contr. Miner. Petrol.* **70**, 143–49.

Kerrick, D. M., & Darken, L. S., 1975. Statistical thermodynamic models for ideal oxide and silicate solid solutions with application to plagioclase. *Geochim. Cosmochim. Acta* **39**, 1431–42.

Laird, J., & Albee, A. L., 1981*a*. High-pressure metamorphism in mafic schist from northern Vermont. *Am. J. Sci.* **281**, 97–126.

—— —— 1981*b*. Pressure, temperature and time indicators in mafic schist: their application to reconstructing the polymetamorphic history of Vermont. *Ibid.* **281**, 127–75.

Leake, B. E., 1978. Nomenclature of amphiboles. *Am. Miner.* **63**, 1023–52.

Marcoux, J., 1978. A scenario for the birth of a new oceanic realm: the Alpine Neotethys. *Abstr. Int. Congr. Sedimentology*, 10th, Jerusalem 1978, Vol. 2, 419–20.

Maruyama, S., Cho, M., & Liou, J. G., 1986. Experimental investigations of blueschist–greenschist transition equilibria: Pressure dependence of Al_2O_3 contents in sodic amphiboles—A new geobarometer. In: Evans, B. W., & Brown, E. H. (eds) *Blueschists and Eclogites. Geol. Soc. Am. Memoir*, **164**, 1–16.

Mather, J. D., 1970. The biotite isograd and the lower greenschist facies in the Dalradian rocks of Scotland. *J. Petrology* **11**, 253–75.

Matthews, A., & Schliestedt, M., 1984. Evolution of the blueschist and greenschist facies rocks of Sifnos, Cyclades, Greece. *Contr. Miner. Petrol.* **88**, 150–63.

Miller, C., 1974. On the metamorphism of eclogites and high grade blueschists from the Penninic terrain of the Tauern Window, Austria. *Schweiz. Miner. Petrogr. Mitt.* **54**, 371–84.

Newton, R. C., 1986. Metamorphic temperatures and pressures of Group B and C eclogites. In: Evans, B. W., & Brown, E. H. (eds) *Blueschists and Eclogites. Geol. Soc. Am. Memoir*, **164**, 17–30.

—— Charlu, T. V., & Kleppa, O. J., 1980. Thermochemistry of the high structural state plagioclases. *Geochim. Cosmochim. Acta* **44**, 933–41.

Okay, A. I., 1978. Sodic pyroxenes from metabasites in the eastern Mediterranean. *Contr. Miner. Petrol.* **68**, 7–11.

—— 1980*a*. Sodic amphiboles as oxygen fugacity indicators in metamorphism. *J. Geol.* **88**, 225–32.

—— 1980*b*. Mineralogy, petrology and phase relations of glaucophane-lawsonite zone blueschists from the Tavşanlı region, northwest Turkey. *Contr. Miner. Petrol.* **72**, 243–55.

—— Özgül, N., 1984. *HP/LT* metamorphism and the structure of the Alanya Massif, southern Turkey: an allochthonous composite tectonic sheet. In: Robertson, A. H. F., & Dixon, J. E. (eds) *The Geological Evolution of the Eastern Mediterranean. Geol. Soc. Lond. Spec. Publ.* **14**, 429–39.

Orville, P. M., 1972. Plagioclase cation exchange equilibria with aqueous chloride solutions. Results at 700 °C and 2000 bars in the presence of quartz. *Am. J. Sci.* **272**, 234–72.

Özgül, N., 1984. Stratigraphy and tectonic evolution of the Central Taurides. In: Tekeli, O., & Göncüoğlu, M. C. (eds) *Geology of the Taurus Belt.* Ankara: Miner. Res. Explor. Inst. Turkey, 77–90.

—— 1985. The geology of the Alanya region (in Turkish). In: *Ketin Symposium.* Geol. Soc. Turkey Publ., 97–120.

Peyronnet, P., 1971. Esquisse géologique de la région d'Alanya (Taurus méridional). Origine des bauxites métamorphiques. *Bull. Miner. Res. Explor. Inst. Turkey* **76**, 90–116.

Ridley, J., 1984. Evidence of a temperature-dependent 'blueschist' to 'eclogite' transformation in high-pressure metamorphism of metabasic rocks. *J. Petrology* **25**, 852–70.

Robertson, A. H. F., & Woodcock, N. H., 1981. Gödene Zone, Antalya Complex: volcanism and sedimentation along a Mesozoic continental margin, SW Turkey. *Geol. Rundschau* **70**, 1177–215.

Schliestedt, M., 1986. Eclogite–blueschist relationships as evidenced by mineral equilibria in high-pressure metabasic rocks of Sifnos (Cycladic islands), Greece. *J. Petrology* **27**, 1437–59.

—— Matthews, A., 1987. Transformation of blueschist to greenschist facies rocks as a consequence of fluid infiltration, Sifnos (Cyclades), Greece. *Contr. Miner. Petrol.* **97**, 237–50.

Selverstone, J., & Spear, F. S., 1985. Metamorphic *P–T* paths from pelitic schists and greenstones from the south-west Tauern Window, Eastern Alps. *J. metamorphic Geol.* **3**, 439–65.

Şengör, A. M. C., & Yılmaz, Y., 1981. Tethyan evolution of Turkey: A plate tectonic approach. *Tectonophysics* **75**, 181–241.

Spear, F. S., Selverstone, J., Hickmott, D., Crowley, P., & Hodges, K. V., 1984. *P, T* paths from garnet zoning: A new technique for deciphering tectonic processes in crystalline terranes. *Geology*, **12**, 87–90.

Thompson, A. B., Lyttle, P. T., & Thompson, J. B. Jr., 1977, Mineral reactions and A–Na–K and AFM facies types in the Gassetts schist, Vermont, U.S.A. *Am. J. Sci.* **276**, 401–24.

Tracy, R. J., Robinson, P., & Thompson, A. B., 1976. Garnet composition and zoning in the determination of temperature and pressure of metamorphism, central Massachusetts. *Am. Miner.* **61**, 762–75.